

# Mechanical and Chemical Properties Of Periodic-Reverse Plated Ni-P Amorphous Alloys

By Robert L. Zeller III and Uziel Landau

A comprehensive study of the mechanical and chemical properties of Ni-P amorphous alloys prepared by various techniques compares the properties of conventionally electroplated amorphous alloys, which are typically quite brittle, to those prepared by a newly developed process. The process is based upon periodic-reverse current (PR) plating, which has been shown to produce electrodeposits with ductility higher, or comparable, to analogous alloys prepared by rapid solidification. The study focuses on determining the effect of PR plating on deposit properties, including ductility, microhardness, hydrogen outgassing, leveling characteristics, corrosion resistance, and the kinetics of hydrogen evolution. Results indicate that the enhanced ductility of the PR-plated alloy does not degrade and may actually improve the important mechanical and chemical properties of Ni-P amorphous alloys.

**A**morphous alloys are attracting considerable interest because of their unique mechanical, chemical, and magnetic properties. Amorphous alloys, also called metallic glasses, have no long-range crystalline order, in contrast to typical metals, which are polycrystalline in form. Because of this glass-like state, their properties are often significantly different from those of the same alloy after crystallization, or by comparison with a polycrystalline alloy of similar composition.

A number of techniques exists to produce amorphous alloys, including rapid solidification, electroless deposition, electrodeposition, sputter deposition, ion implantation, and laser glazing. Electrodeposition provides a convenient method for producing these alloys because it offers a relatively inexpensive, one-step technique to form monolithic parts from amorphous alloys with appreciable thickness and controlled shape. It can also be used to plate parts with thin amorphous alloy coatings for corrosion protection and hardness. Amorphous alloys prepared by conventional electrodeposition are, however, extremely brittle, as compared to the analogous material prepared by rapid solidification.

We have shown earlier<sup>1</sup> that electrodeposited Ni-P amorphous alloys do not exhibit classical hydrogen embrittlement. Instead, features of the microstructure, principally the presence of voids, have been implicated as the major cause of brittleness. We have recently developed a process,<sup>2</sup> based on periodic-reverse current (PR) plating, which produces significantly more ductile electrodeposits than the comparable material prepared by conventional electrodeposition. Analysis indicates that the microstructure of the PR-plated alloys is quite different from that prepared by conventional direct current (DC) or pulse plating (PP) processes.<sup>2</sup>

The purpose of this study was to analyze the mechanical and chemical properties of the amorphous Ni-P alloys electrodeposited by the PR process and determine whether these are different from the conventional DC-plated material. Specifi-

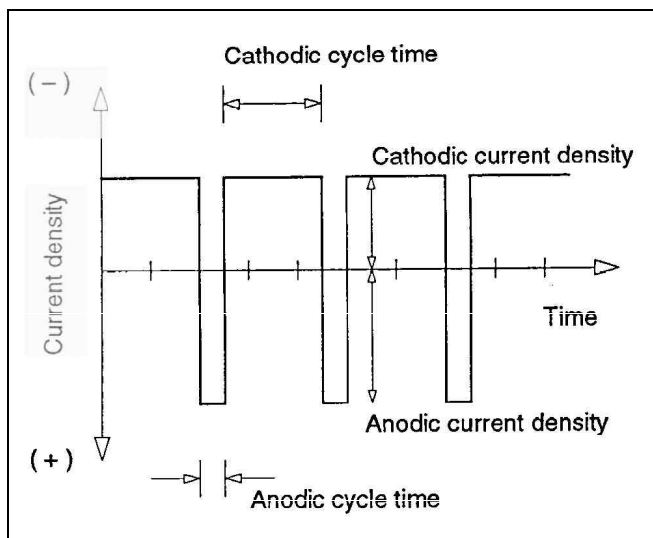


Fig. 1—Typical current wave form for periodic-reverse (PR) plating.

cally, the ductility, microhardness, hydrogen outgassing, leveling characteristics, corrosion resistance, and hydrogen evolution kinetics were investigated.

## Experimental Procedure

The alloys were electrodeposited on a rotating disk electrode (RDE) at a rotation rate of 2000 rpm from a bath with the composition and operating conditions as listed in Table 1. All solutions were prepared using distilled-deionized water and analytical grade chemicals. The PR-plated alloys were prepared using the current waveform presented in Fig. 1. The cathodic and anodic current densities and cycle times were varied as listed in Table 1. The composition of the DC-plated alloy was 23.6 atomic percent P; the PP alloy was 23.6 atomic percent P; the PR 8:1 (ratio of cathodic to anodic cycle times: 8:1) alloy was 26.6 atomic percent P; and the PR 6:1 (ratio of cathodic to anodic cycle times: 6:1) was 26.2 atomic percent P. The composition of the alloys was determined using Energy Dispersive Spectrography (EDS). Further details concerning the electrodeposition and analysis techniques may be found in Ref. 1.

The properties of the electrodeposited alloys were measured and compared to that of MBF-60.<sup>3</sup> This commercially available Ni-P alloy is prepared by melt-spinning and has a composition of approximately 19.5 atomic percent P.

The ductility of the alloys was measured by a mechanical bulge tester and by bend testing. Details of the ductility testing techniques are also given in Ref. 1.

Microhardness measurements were conducted using a hardness tester<sup>4</sup> equipped with a Vickers diamond indenter under a 50-g load. Three measurements were always averaged. The back side of the electrodeposit showed no mechani-

**Table 1**  
**Ni-P Electroplating Bath Composition and Operating Conditions**

Bath Composition					
	NiSO <sub>4</sub> •6H <sub>2</sub> O	150.0 g/L			
	NiCl <sub>2</sub> •6H <sub>2</sub> O	45.0 g/L			
	H <sub>3</sub> PO <sub>3</sub>	40.0 g/L			
	H <sub>3</sub> PO <sub>4</sub>	40.0 ml/L (0.69M)			
	pH adjusted to (using KOH)	1.00 to 1.45			
Operating Conditions					
	DC	PP	PR 8:1	PR 6:1	Units
Temperature	85	85	85	85	°C
Cathodic cd.	-0.25	-0.25	-0.25	-0.25	A/cm <sup>2</sup>
Cathodic time	N/A	0.6	0.8	0.6	sec
Anodic c.d.	N/A	0	0.6	0.25	A/cm <sup>2</sup>
Anodic time	N/A	0.1	0.1	0.1	Sec

cal deformation because of the indenter. The microstructure of the electrodeposited alloys was compared qualitatively by differential scanning calorimetry (DSC)<sup>6</sup> at a rate of 20 °C/min. The microhardness was also measured on some of the samples which were crystallized during the DSC analysis.

Hydrogen out-gassing tests were performed, using Low Temperature Vacuum Annealing (LTVA) on DC- and PR-plated alloys at 102 °C, following the procedure of Okinaka and Straschil.<sup>3</sup> Essentially, the total hydrogen content was measured as a function of annealing time, using a hydrogen determinator.<sup>4</sup> The data were then fitted to a theoretical model<sup>5</sup> which provides the effective diffusion coefficient of hydrogen, D.

The leveling characteristics of the bath were determined for DC and PR 6:1 plating processes, with the respective operating conditions listed in Table 1. The leveling characteristics were quantified by electroforming the amorphous deposit on a modulated substrate and measuring the change in the surface modulation. The surface profiles were measured using an alpha-step thin film and surface profile measurement system.<sup>9</sup> The substrate was made of OFHC copper and was mounted on the RDE system. The rotation rate was sufficient to preclude hydrogen gas bubbles adhering to the substrate. The alloys were plated for eight hours in a bath similar to that described in Table 1, with the pH adjusted to 1.35.

The corrosion resistance was qualitatively determined by steady-state anodic polarization in aerated 0.05 N HCl with a pH of 1.33. The counter electrode was either a graphite rod or a platinum mesh. The choice of counter electrode did not influence the anodic polarization curves. All potentials were corrected for IR drop. Prior to the corrosion test, the electrode was polarized -0.7 V vs. SCE to reduce possible air-formed oxide layers and the system was allowed to reach steady-state (approximately 3 to 5 rein). The electrode was then polarized to -0.3 V vs. SCE, allowed again to reach steady-state, and 100 current measurements were taken over 50 sec. The high and low currents were recorded. The electrode was then repeatedly stepped 0.05 V anodic and, after 20 sec, 100 current measurements were taken. Each potential step required approximately 100 sec to measure, corresponding to an effective voltage sweep rate of 0.5 mV/sec. The nickel electrode was a cold-rolled 99.99 percent nickel foil.

The kinetics for hydrogen evolution were determined by cathodically polarizing the electrode in 0.05 N HCl and measuring the steady-state current. Hydrogen gas was bubbled to ensure saturation and to de-aerate the system. Potential steps of -0.01 to -0.025 V were applied in the cathodic direction, starting from the open circuit potential (1 = 0). Prior to testing, the electrode was polarized -0.7 V vs. SCE for 30 sec, to reduce any air-formed oxide film.

## Results and Discussion

### Ductility and Microstructure

A detailed study and specific discussion of the ductility and microstructure of the PR-plated amorphous alloy can be found in Ref. 2. In summary, the ductility of the PR-plated alloy is much higher than that of the DC material and actually equals or exceeds that of MBF-60, used as a ductility comparison reference. This enhanced ductility is indicated in Fig. 2, which shows the ductility (in percentage elongation) and the bend test angle as a function of deposit thickness for DC- and PR 8:1-plated alloys. The microstructure of the PR-plated material was shown to contain no voids and consisted of two interleaving phases: One essentially identical to that produced by DC or PP electrodeposition, and another which is less conductive and exhibits reduced thermal stability.

### Microhardness

The microhardness data, along with the total hydrogen content and ductility of the DC and PR 8:1-plated alloys and the MBF-60 samples are summarized in Table 3. As shown, with micro hardness similar to that of the as-plated DC materials, the ductility of the PR 8:1 (as-plated) material approaches that of the MBF-60. The microhardness of the crystallized alloys

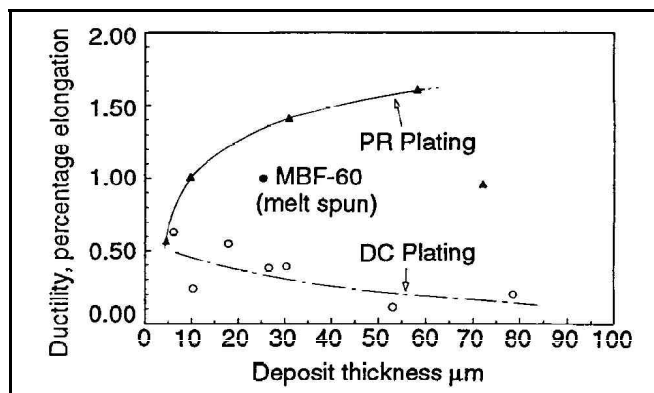


Fig. 2a—Ductility in percentage elongation as a function of deposit thickness. O = DC; ▲ = PR 8:1; ● = MBF-60

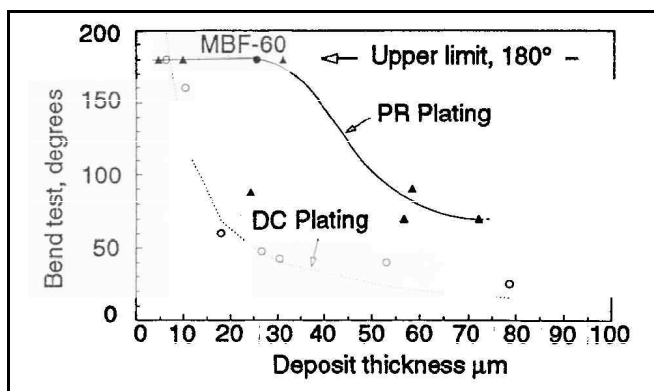


Fig. 2b—Bend test in angle at fracture as a function of deposit thickness. O = DC; ▲ = PR 8:1; ● = MBF-60

**Table 2**  
**Physical Properties of Alloys\***

Forming Process	H content (at %)	Ductility		Hardness (VHN, kg/mm <sup>2</sup> )	
		% elongation	bend test	As plated	Crystallized
DC Plating	0.723	<0.5%	<50°	520 ± 62	891 ± 55
PR (8:1) Plating	1.476	>1.0%	180°	580 ± 7	845 ± 55
MBF-60 (melt-quenched)	0.085	1.0%	180°	500 ± 50	877 ± 15

\*All at same sample thickness (~25 μm).

**Table 3**  
**Average Kinetic Parameters For Hydrogen Evolution**

	$i_0$ (μA/cm <sup>2</sup> )	$\beta_c$ (mV/decade)	$V_{\infty}$ (V vs SCE)
DC	4.4 ± 0.5	112 ± 0.3	0.105
PP	11.9 ± 4.0	164 ± 29	0.080
PR 6:1	6.5 ± 4.3	164 ± 35	0.040
PR 8:1	9.9 ± 3.0	171 ± 20	0.055
MBF-60	5.6 ± 1.1	123 ± 3	0.110
Nickel Foil	51.8 ± 16.4	212 ± 60	0.200
Type 4340 Steel	193.6 ± 35.6	42 ± 2	0.520

(obtained after the DSC analysis) are also presented in Table 2. As shown, the hardness increases significantly after the alloy is crystallized. The values for hardness of the amorphous and crystallized Ni-P alloys compare well with data presented in the literature.<sup>4,5</sup>

The effect of annealing on microhardness is presented in Fig. 3 for PR 8:1 -and DC-plated alloys. As shown, the microhardness of the PR 8:1 alloy increases with annealing time. This is probably a result of crystallization processes in the PR 8:1 alloy. DSC analysis indicates that the microstructure of the PR 8:1-plated alloy does change with annealing time.<sup>2</sup> By contrast, the DC-plated alloy exhibited invariant DSC curves over the entire annealing process, indicating that no microstructural changes took place. The temperature dependence of the PR 8:1 alloy may be an advantage, in that a lower temperature is required to crystallize the material and obtain a much harder coating. Also, the results indicate that microhardness can be controlled to tailor it to specific applications. After the PR 8:1 alloy was annealed for a short period of time, however, its ductility decreased and approached that of the DC-plated alloy. This is probably because of partial and selective crystallization within the PR 8:1 electrodeposit.

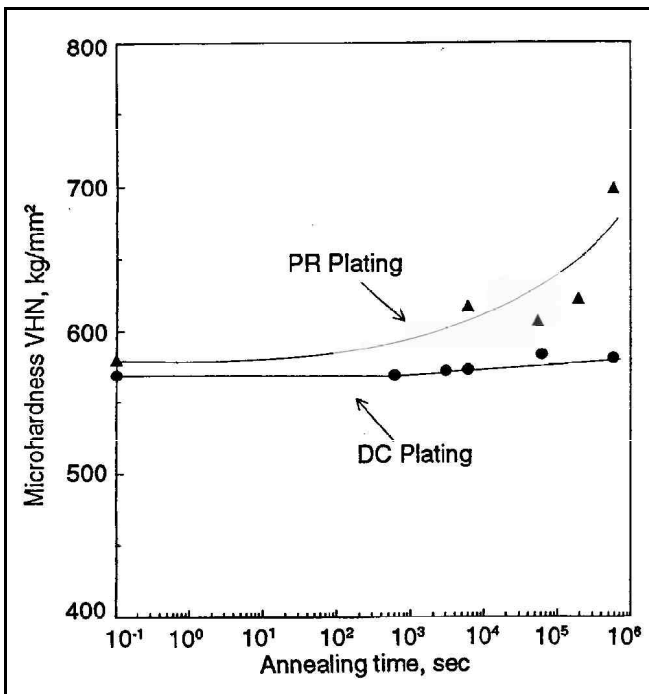


Fig. 3—Vickers hardness as a function of annealing time (at 102°C) for DC and PR 8:1 electrodeposited Ni-P alloys. ● = DC; ▲ = PR 8:1.

#### Hydrogen Outgassing

The results of the LTVA experiments are shown in Fig. 4 for both the PR 8:1- and DC-plated materials. As shown, all of the hydrogen in both alloys is diffusible. The effective diffusion coefficient for hydrogen in the PR-plated alloy is almost two orders of magnitude smaller than that of the DC-plated alloy. Unlike the DC-plated alloy, the DSC curves of the PR 8:1-plated alloy exhibit changes in crystallization processes, indicating a change in microstructure. We have hypothesized that the hydrogen in the PR 8:1 alloys may stabilize the amorphous structure, and that it is probably "bound to the Ni-P alloy. Therefore, it is difficult to interpret the effective diffusion coefficient for the PR 8:1-plated alloy quantitatively.

#### Leveling Characteristics

In order to determine the effects of the process parameters on the surface texture of the deposit and the capability of the process to produce relatively thick, yet smooth and level electroforms, a number of long plating experiments was conducted. To obtain a critical measure of the leveling characteristics, triangular grooves (0.1 mm) were milled into the OFHC copper substrate. Typical surface profiles of the substrate,

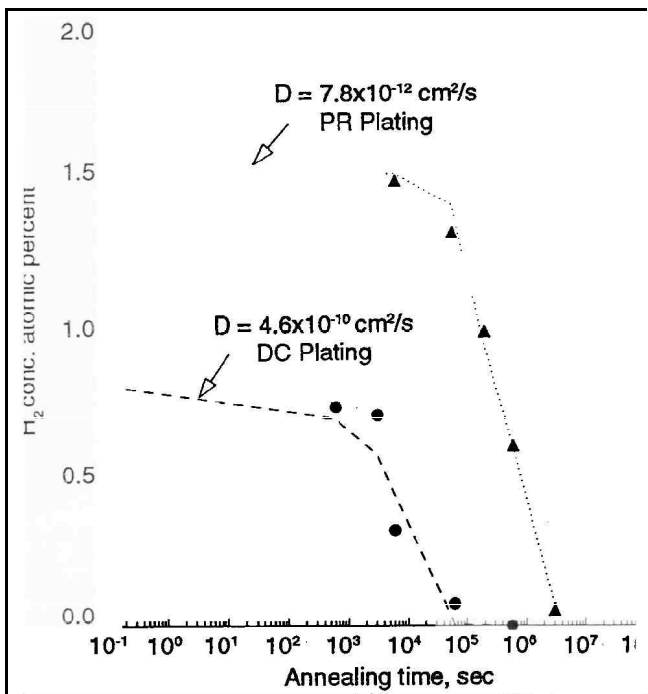


Fig. 4—Hydrogen content as a function of annealing time (at 102°C) for DC and PR 8:1 electrodeposited Ni-P alloys. ● = DC; ▲ = PR 8:1.

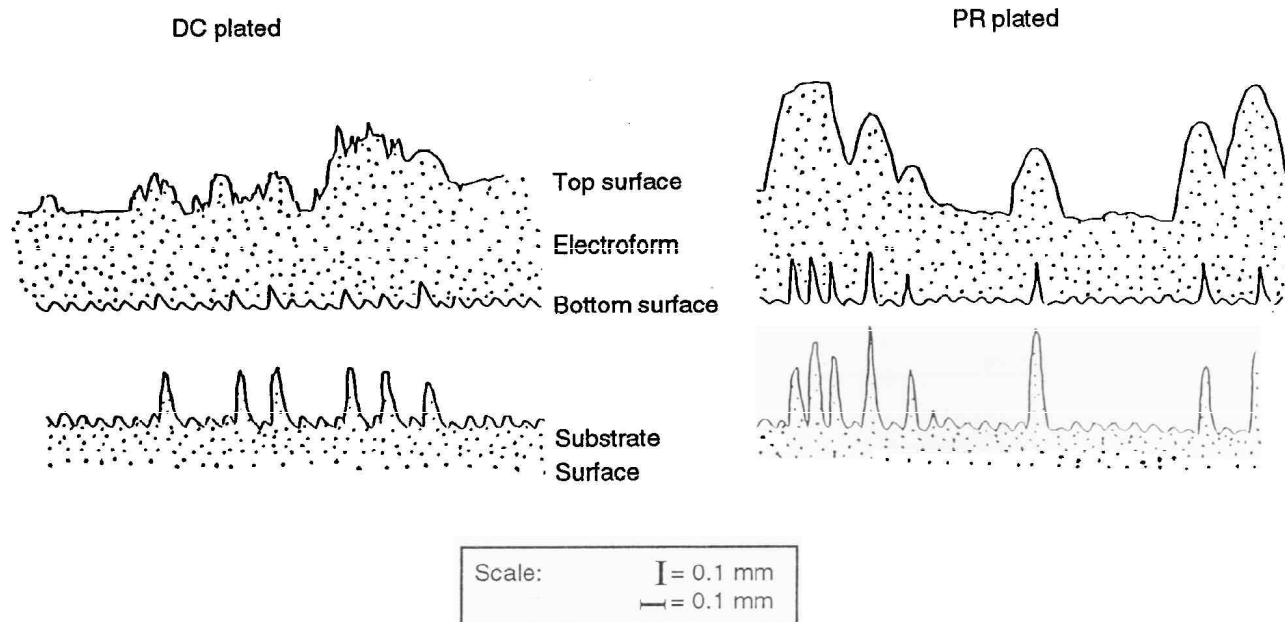


Fig. 5-Representative deposit texture illustrating surface topology for (a) DC and (b) PR 6:1 electrodeposited alloys.

electrodeposit-substrate interface, and the top surface of the electrodeposit for the DC- and PR 6:1-plated materials are shown in Fig. 5. The distortion of the surface profile from perfect triangles can be attributed to limitation in penetration of the mechanical tracing device (tip radius of 5  $\mu\text{m}$ ). As noted from Fig. 4, the notches in the bottom surface of the electroformed alloy correspond in position to the substrate protrusions. The discrepancy in the depth of the groove (as compared to the substrate) can again be attributed to limitation in penetration of the mechanical tracing device.

It is noted that in both plating processes, the smaller perturbations are dampened and the larger perturbations are amplified with deposition. The DC data show, however, a much coarser surface, while the PR 6:1 surface is quite smooth on the micro-scale. This indicates that PR plating provides much better micro-leveling than the DC process. Similar phenomena have been previously noted for PR and PP in copper electrodeposition.<sup>5</sup>

The surface profiles on the macroscale can be quantified in terms of stability criteria proposed by Shyu and Landau,<sup>7</sup> to indicate the macroleveling characteristics of the processes. Accordingly, the ratio,  $\delta/\dot{\delta}$ , quantifies whether the system is unstable with respect to surface perturbations. The quantity  $\delta$  is the initial height of the perturbation and  $\dot{\delta}$  denotes its rate of change,  $d\delta/dt$ . A positive  $\delta/\dot{\delta}$  ratio indicates that the surface perturbations grow at a faster rate than the surface as a whole; when negative, the deposition exhibits good macroleveling properties. The estimated ratios from the surface profiles are  $0.025 \pm 0.069/\text{hr}$  for the DC process and  $0.057 \pm 0.076/\text{hr}$  for the PR 6:1 process. As noted, the ratios for the PR 6:1-plated alloy are larger than that of the DC process (although both are positive), indicating poor macroleveling characteristics. The large standard deviations indicate that the propagation rates of the large features can be quite different.

This difference in the macroleveling characteristics between DC- and PR-plating maybe related to mass transfer effects associated with the PR process or to a coupled current distribution-anodic film formation phenomenon. Simple

analysis indicates that mass transfer effects are unlikely to be significant because the time scale for fully developed concentration profiles is one to two orders of magnitude shorter than the cathodic on-time.

Current distribution variations, coupled with the formation of corrosion products on the surface, may cause the observed macroleveling characteristics. As noted from the leveling characteristics of the DC process, the Ni-P deposition is intrinsically unstable (i.e., surface perturbations tend to grow faster than the adjacent surface). Upon passing an anodic current, we would expect enhanced dissolution of material from the perturbation tip, because of its greater accessibility, resulting in smoother surfaces. The Ni-P amorphous alloy forms an anodic film on the surface,<sup>\*</sup> however, which may lead to more uniform dissolution from the substrate. It would be expected that a thicker anodic film would form at the tip than on the surrounding surface, because of the increased local anodic current density at this location. Because we have postulated that the anodic film formed during the anodic current cycle is redeposited at the start of the cathodic current cycle, this will lead to increased deposit thickness at the tip. Thus, the tip growth velocity would be greater for the PR process than the DC process as a result of the coupled effect of current distribution and the formation on a non-uniform anodic film, which is redeposited upon return to the cathodic current.

#### Corrosion Resistance

Anodic polarization experiments were conducted on DC, PP, PR 6:1, and PR 8:1-plated alloys, MBF-60, and nickel in 0.05 N HCl. The anodic polarization curves are presented in Fig. 6. As noted, all of the Ni-P alloys exhibit similar corrosion resistance. The polarization curves are similar to those presented by other researchers.<sup>8-10</sup> The slight variations in the anodic polarization characteristics of the Ni-P alloys may be attributed to differences in the phosphorus mole fraction in the alloy.<sup>9</sup> Therefore, it maybe concluded that PR plating does not significantly alter the corrosion resistance, as compared to the DC-plated alloy.

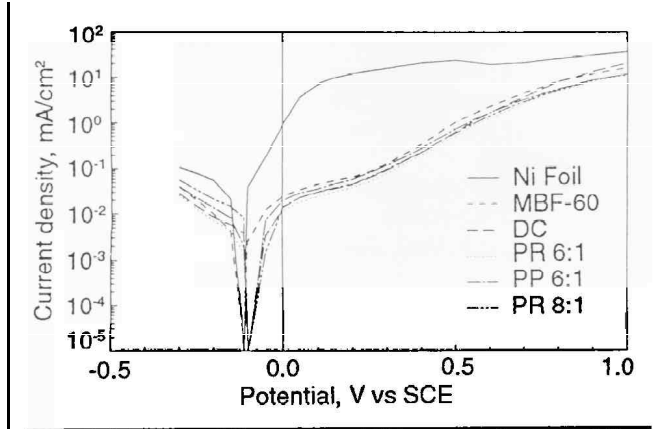


Fig. 6—Anodic polarization curves in 0.05 N HCl for nickel, MBF-60, C, PP, PR 6:1, and PR 8:1 Ni-P alloys.

In contrast, the pure nickel electrode exhibited anodic currents which were over a broad potential range two to three orders of magnitude higher than those for the Ni-P alloys, indicating a less passive nature. The nickel electrode was found to be covered by a loosely adhering black film, but no such film was observed on the Ni-P alloys.

The surfaces of the electrodes were examined for pitting after the tests. All of the nickel foil, MBF-60, and the DC- and PP-plated films exhibited pitting of varying degrees, however, the PR-plated alloys showed no pitting. Although this result is qualitative, it may indicate that the layered structure of PR plating may help eliminate pitting in Ni-P alloys.

#### Kinetics of Hydrogen Evolution

The kinetics of hydrogen evolution were measured on DC, PP, PR 6:1, and PR 8:1-plated alloys, MBF-60, nickel, and on Type 4340 steel for comparison. The determination of the precise hydrogen kinetic mechanism of adsorption, charge transfer, recombination, and desorption was not attempted. The kinetic parameters determined here, however, are useful from an engineering perspective. The kinetics of hydrogen evolution may be technologically significant because Ni-P coatings on steel have been proposed as a hydrogen embrittlement barrier.<sup>11</sup> It has been suggested that the important parameter associated with hydrogen embrittlement is the exchange current density for hydrogen evolution on the coating.<sup>11</sup> The two-orders-of-magnitude-lower diffusion coefficient of the PR-plated alloy (in comparison to the DC-plated alloy), as discussed earlier, may further enhance the usefulness of the PR-plated alloy as a hydrogen embrittlement barrier. Type 4340 steel was tested because it is highly susceptible to hydrogen embrittlement and is a possible candidate for Ni-P coatings. In addition to the barrier application, some amorphous alloys were reported to exhibit, in general, unique and attractive catalytic properties.<sup>12</sup>

A typical cathodic polarization curve is shown in Fig. 7. The data were analyzed to provide estimated exchange current densities and Tafel slopes, and the results, together with their standard deviations, are summarized in Table 3. As noted, the kinetics of hydrogen evolution are similar for all Ni-P alloys and are about one order of magnitude slower than that for pure nickel. This is in contrast to Moffat et al.,<sup>13</sup> who report that nickel alloyed with phosphorus increases the exchange current density of the hydrogen evolution reaction. The values of the exchange current densities for the Ni-P alloys are similar to those presented by Moffat et al. for melt-quenched Fe<sub>80</sub>B<sub>20</sub> in 1 N HCl.

As shown, the exchange current densities of the Ni-P alloys

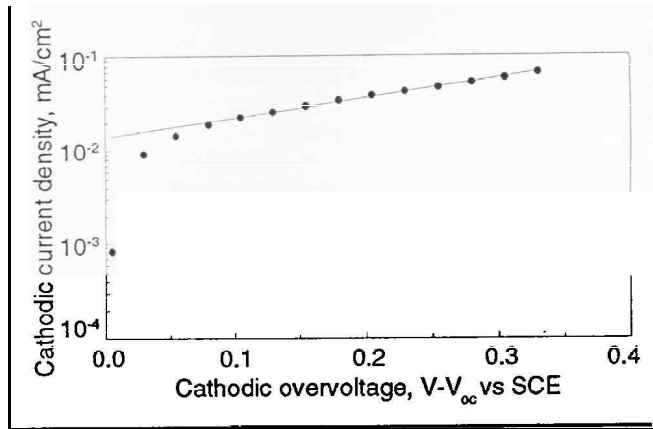


Fig. 7—Typical cathodic polarization curve for determination of hydrogen kinetic parameters showing the Tafel region (PR 6:1 in 0.05 N HCl).

are two orders of magnitude lower than that of Type 4340 steel. Wilde et al.<sup>11</sup> have shown that the exchange current density is the most important parameter for hydrogen embrittlement barriers. In addition to the exchange current density difference, the Tafel slopes for the Ni-P alloys are much greater than those of Type 4340 steel ( $\approx 170$  vs.  $42$  mV/decade). Thus, the rate of hydrogen evolution is significantly decreased on the Ni-P alloys. The open circuit potential ( $i = 0$ ) for the Ni-P alloys was more than 400 mV noble compared with Type 4340 steel (Table 3).

Using the best fit kinetic parameters given in Table 3, which were averaged from numerous experiments, reconstructed cathodic polarization curves for each alloy are illustrated in Fig. 8. As shown, the electrodeposited Ni-P alloys exhibit nearly identical cathodic polarization behavior. The melt-quenched Ni-P amorphous alloy (MBF-60) has kinetics similar to the electrodeposited alloys, but its open circuit potential is approximately 100 mV more cathodic. This may be a result of differences in the alloy composition or differences in microstructure. The cathodic polarization curve for Type 4340 steel is presented for comparison. It may, therefore, be concluded that electrodeposited Ni-P amorphous alloys are promising candidates for both a hydrogen embrittlement barrier and a highly effective corrosion-resistant coating.

#### Conclusions

Periodic Reverse plating produces a much more ductile material than comparable alloys obtained by the conventional (DC or PP) electroplating process. The thermal stability of the PR alloys is not as great as that of the DC-or PP-plated alloys. This could, however, be used to advantage by providing means of

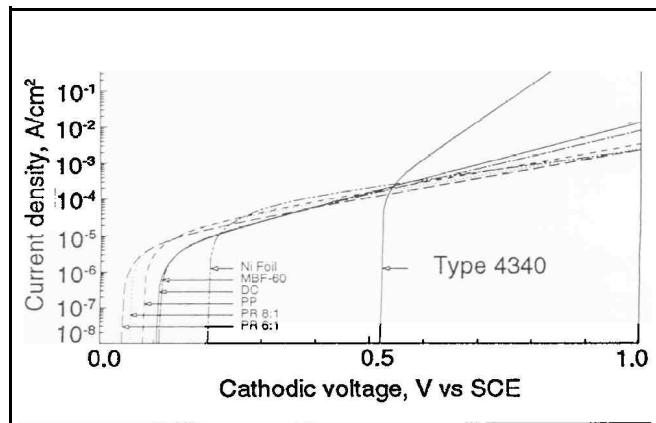


Fig. 8—Reconstructed cathodic polarization curves using best fit kinetic parameters (from Table 3) for DC, PP and PR plated Ni-P amorphous alloys, a melt-quenched Ni-P amorphous alloy (MBF-60), nickel foil and Type 4340 steel.

increasing the microhardness at moderate temperatures. Nee and Weil,<sup>a</sup> in a more thorough investigation, found that pulsed plating had little effect on the mechanical properties of electrodeposited Ni-P alloys, as compared to the same alloy prepared by conventional DC plating.

The mechanical and chemical properties of amorphous alloys produced by the PR process are not significantly different from those of the DC- or PP-plated material and some of the desirable properties are actually enhanced.

<sup>a</sup>Allied Metglas Products, Parsippany, NJ.

<sup>b</sup>Model 3212, Zwick of America, Inc., East Windsor, CT.

<sup>c</sup>Model DSC 7, Perkin-Elmer Corp., Norwalk, CT.

<sup>d</sup>Model RH-2, LECO Corp., St. Joseph, MI.

<sup>e</sup>Tencor Instruments, Mountain View, CA.

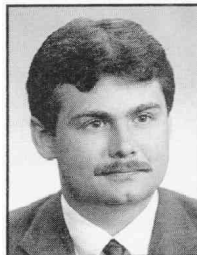
## Acknowledgments

This work was conducted with the support of the Aluminum Company of America (Alcoa). Useful discussions with Alfred F. LaCamera are acknowledged. The American Electroplates and Surface Finishers Society is acknowledged for providing a supplemental fellowship to R.L. Zeller.

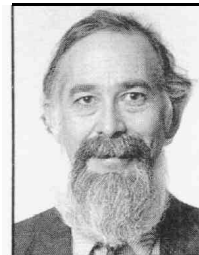
## References

1. R.L. Zeller III and U. Landau, *J. Electrochem. Soc.*, 137, 1107 (1990).
2. R.L. Zeller III and U. Landau, *ibid.*, 138,1010 (1991).
3. Y. Okinaka and H.K. Straschil, *ibid.*, 133,2608 (1986).
4. D.S. Lash more and J.F. Weinroth, *Plat. and Surf Fin.*, 69, 72 (Aug., 1982).
5. R. Weil, J.H. Lee, I. Kim and K. Parker, *ibid.*, 76,62 (Feb., 1989).
6. J.R. White and R.T. Galasco, *ibid.*, 75,122 (May, 1988).
7. J.H. Shyu and U. Landau, Electric Power Research institute Report EM-2937 (1983).
8. R.B. Diegle, N.R. Sorensen, C.R. Clayton and M. Helfand, *Corrosion, Electrochemistry, and Catalysis of Metallic G/asses*, R.B. Diegle and K. Hashimoto, Eds., The Electrochemical Society, 88-1, 80 (1 988).
9. M. Ratzker, D.S. Lashmore and K.W. Pratt, *Plat. and Surf. Fin.*, 73,74 (Sept., 1986).
10. P.V. Nagarkar, P.C. Searson and R.M. Latanision, *Corrosion, Electrochemistry, and Catalysis of Metallic Glasses*, R.B. Diegle and K. Hashimoto, Eds., The Electrochemical Society, 88-1, 118 (1988).

11. B.E. Wilde, M. Manohar, I. Chattaraj, R.B. Diegle and A.K. Hays, *Corrosion, Electrochemistry, and Catalysis of Metallic Glasses*, R.B. Diegle and K. Hashimoto, Eds., The Electrochemical Society, 88-1,289 (1988).
12. M.D. Archer, C.C. Cocke and B.H. Harji, *Electrochimica Acta*, 32, 13 (1987).
13. T.P. Moffat, W.F. Flanagan and B.D. Lichter, *J. Electrochem. Soc.*, 135,2712 (1988).
14. C.C. Nee and R. Weil, *Surface Technology*, 25,7 (1985).



Zeller



Landau

## About the Authors

**Dr. Robert L. Zeller III** is a senior research engineer with Occidental Chemical Corporation, 2801 Long Rd., Grand Island, NY 14072, investigating the technology of chromium chemicals manufacture and their applications. He holds a BS and an MS in chemical engineering from the University of Akron and a PhD in chemical engineering from Case Western Reserve University He has received two AESF scholarships and has worked on AESF Reseach Project 65.

**Dr. Uziel Landau** is professor of chemical engineering at Case Western Reserve University. His research activities focus on theoretical and experimental aspects of electroplating, including alloys and novel compound deposition, roughness inhibition, and predictive modeling of current and deposit thickness distribution in electrochemical cells. Dr. Landau holds BSc and MSc degrees in chemical engineering from the Technion (Israel Institute of Technology), Haifa, and a PhD from the University of California at Berkeley.